CHAPTER IV

INFLUENCE OF COPPER OXIDE NANOPARTICLES ENSEMBLED ON CHITOSAN BLENDED REDUCED GRAPHENE OXIDE NANOSHEETS FOR THE ELECTROCHEMICAL DETECTION OF p-AMINOPHENOL

4.1 INTRODUCTION

In general the contaminants and unwanted molecules are needed to be accurately controlled and minimized to provide a safe and trustable product. p-Aminophenol (p-AP), a well known organic compound used as an intermediate product for the preparation of drugs, chemicals etc., p-AP is an environmental pollutant used in various industrial fields such as petroleum, dye and medicine [1]. Moreover, the accumulation of p-AP in environment leads to serious disorders such as kidney damage, liver disorders, skin rashes, inflammation of the pancreas and may even lead to death. Due to its significant effects, the excessive residual of p-AP in environment should be strictly controlled [2]. Many methods have been used for the determination of p-AP. Among all these methods, electrochemical sensing is chosen to be the best method due to its low cost, fast determination and high sensitivity [3].

Graphene is a two dimensional sp^2 hybridized carbon atom packed in a honeycomb network. The properties of graphene oxide can be effectively modified by modifying it with the functional nanomaterials such as polymers, metals and catalysts in order to produce a versatile electrochemical sensing performance [4-5]. Chitosan (CS) is a linear β-1,4-linked polyaminosaccharide natural bio polymer. Due to its extraordinary properties like good adhesion and mechanical strength it is used as an ideal material in sensing applications. The hydroxyl and amino group of CS helps in the chemical modification of nanomaterials by interacting with metals or metal oxides which results in the enhancement of properties. Incorporation of nanoparticles into the polymer matrix has become an active arena of research due to their promising application in versatile fields [6]. Among various metal nanoparticles, copper nanoparticles (Cu NPs) have been widely used in many fields

due to their excellent physical and chemical properties, easy preparation and the low synthetic cost [7-8].

Hence, in this chapter a facile chemical reduction method is used for the synthesis of rGO/CS/CuO nanocomposites. The synthesized nanocomposites are characterized by FT-IR, XRD, SEM, EDAX, TEM, SAED analysis. The samples are tested for the electrochemical detection of p-Aminophenol and optimized using various pH and scan rate.

4.2. EXPERIMENTAL PROCEDURE

4.2.1. Reagents

Graphite powder, conc.sulphuric acid (98%H_2SO_4), potassium permanganate ($KMnO_4$), hydrogen peroxide solution (30% H_2O_2), sodium nitrate ($NaNO_3$), sodium hydroxide (NaOH), copper II acetate monohydrate($CH_3COO_2C_4.H_2O$), sodium borohydride ($NaBH_4$) and p-aminophenol are of analytical grade, purchased from sigma Aldrich and are used as received without further purification.

4.2.2. Synthesis of reduced graphene oxide / chitosan / copper oxide nanocomposites

The rGO / CS/ CuO nanocomposites are synthesized by dispersing 50 mg of rGO/CS solution in 25 ml of distilled water by ultrasonication for 1 hour to form the aqueous rGO/CS solution. About 0.002 M of Copper II acetate monohydrate is taken in 50 ml of distilled water and stirred for 1 hour seperately. The stirred Copper II acetate monohydrate solution is added dropwise into the above dispersed rGO/CS solution under constant stirring. Then 25 mg of $NaBH_4$ is taken in 50 ml of distilled water and stirred for 1 hour separately. The stirred $NaBH_4$ solution is added drop wise and stirred for 4 hours at 60°C. The formed solution is left undisturbed for overnight and the resultant supernatant is filtered and washed rigorously by centrifuging at 8000 rpm. It is then dried in oven at 60°C for 4 hours and the sample is grinded finely to form the rGO/CS/CuO nanocomposites [9-10]. Similiar procedure is followed to prepare various concentrations of Copper II acetate monohydrate (0.004 M, 0.006 M, 0.008M and 0.01M) to form rGO/CS/CuO nanocomposites.

4.3 RESULTS AND DISCUSSION

4.3.1 FT-IR spectral analysis

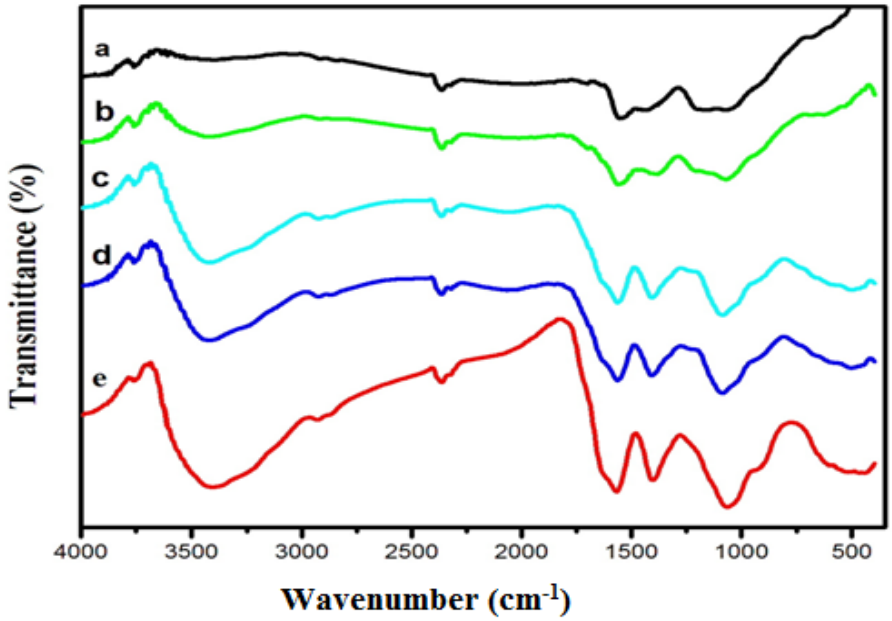

Figure 4.1 (a-e) FT-IR spectral analysis for various concentrations (a) 0.002 M (b) 0.004 M (c) 0.006 M (d) 0.008 M and (e) 0.01 M of copper oxide nanoparticles on the surface of rGO/CS nanocomposites

The structural and bond information of the prepared nancomposites is indentified using FT-IR spectral analysis. Figure 4.1 (a-e) shows the FT-IR spectral analysis for various concentrations of monohydrate (0.002 M, 0.004 M, 0.006 M, 0.008 M and 0.01 M) Copper II acetate on the surface of rGO/CS nanocomposites. It is observed from the Figure 4.1 (a-e), that the wide absorption band at 3413 cm^{-1} corresponds to the O-H stretching vibrations of water molecules overlapping with N-H stretching vibrations of amino group. The sharp intense band at 1569 cm^{-1} attributes to the carbonyl stretching vibrations of secondary amide groups. The band at 1042 cm^{-1} attributes to the C-O stretching vibrations of primary alcohol. The absorption band at 1407 cm^{-1} corresponds to the C-O stretching vibrations of carboxyl group of chitosan. In particular, the metal-oxygen (Cu-O) vibration band is observed around 486 cm^{-1} [11].

It is further observed that on increasing the concentration of copper II acetate monohydrate from 0.002 M to 0.01 M, the intensity of the band of rGO/CS/CuO nanocomposites also increases. The increase in width of the band at 3413 cm^{-1} indicates the intermolecular hydrogen bonding with O-H groups [12]. This increase in the intensity of the bands is due to the strong interaction of hydrophilic nature of chitosan with copper oxide nanoparticles. This demonstrates that copper oxide nanoparticles have been successfully formed into the reduced graphene oxide/chitosan matrix.

4.3.2 XRD Structural Analysis

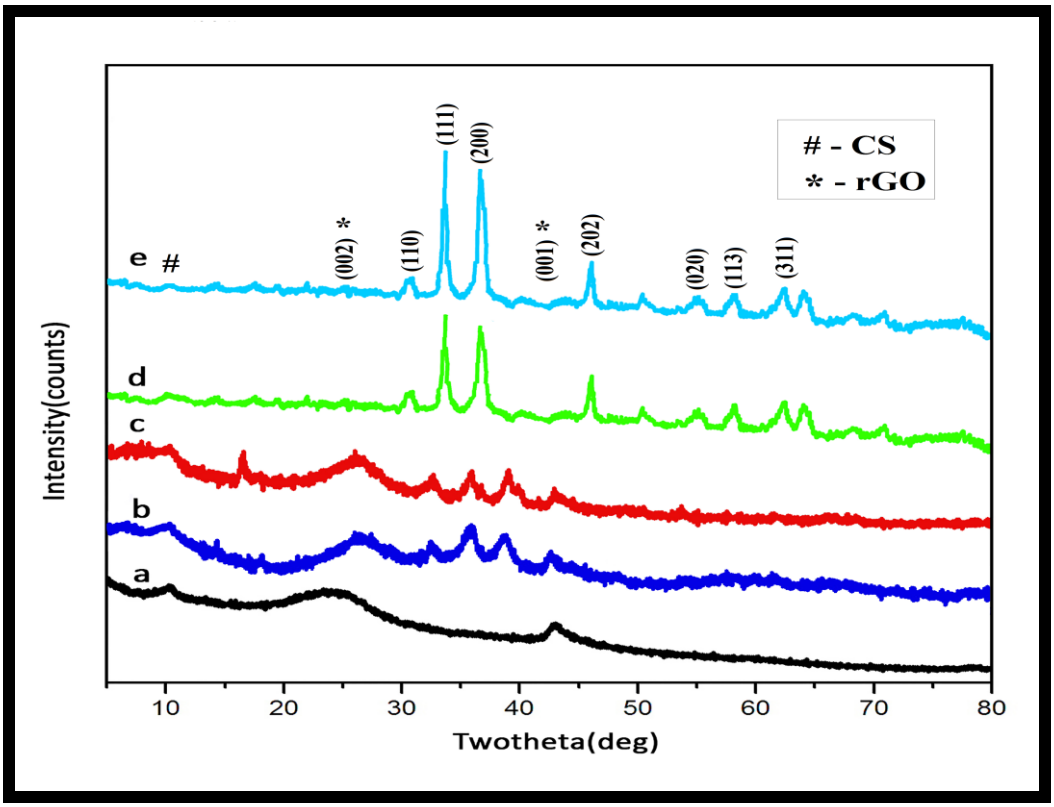

Figure 4.2 (a-e) XRD pattern for various concentrations (a) 0.002 M (b) 0.004 M (c) 0.006 M (d) 0.008 M and (e) 0.01 M of copper oxide nanoparticles on the surface of rGO/CS nanocomposites

The crystalline nature of the prepared rGO/CS/CuO nanocomposites at different concentrations is studied using XRD. Figure 4.2 (a-e) shows the XRD pattern for various concentrations of copper II acetate monohydrate 0.002 M, 0.04

M, 0.006 M, 0.008 M and 0.01 M on the surface of rGO/CS nanocomposites. It is observed from the Figure 4.2 (a) that the peak at 10.9^{o} corresponds to the plane of chitosan. The broad peak at 24.5^{o} corresponds to the (002) plane of reduced graphene oxide and the small additional peak at 42^{o} corresponds to the (001) plane that may be due to the incomplete oxidation of graphite. The broadness of the peak at 24.5^{o} is due to blending of chitosan into reduced graphene oxide which thereby increases the inter layer spacing of reduced graphene oxide nanosheets. It is observed from the Figure 4.2 (b-e) that the diffraction peaks positioned at 31.5˚, 35.6˚, 38.7˚, 48.7˚, 53.6˚, 57.9˚, 61.4˚ and 66.1˚ corresponds to the (110), (111), (200), (202), (020), (021), (113) and (311) planes of monoclinic phase of copper oxide nanoparticles which are well indexed with the standard JCPDS card number 48-1548 [13-14]. Figure 4.2 (a) clearly depicts that due to low concentration of copper II acetate monohydrate (0.002 M), no diffraction peaks of copper oxide nanoparticles is observed, thereby indicating the strong binding of chitosan into the rGO. But by increasing the concentration of Copper II acetate monohydrate from 0.004 M to 0.01M, the intensity of diffraction peaks of copper oxide nanoparticles increases with decrease in the intensity of diffraction peaks of rGO/CS.

The crystallite size is calculated using Debye Scherrer's formula and is found to be about 9.6 nm, 10.8 nm, 12.7 nm, 16.1 nm and 18.5 nm for various concentrations of rGO/CS/CuO nanocomposites respectively. The crystallite size of copper oxide nanoparticles increases on increasing the concentration of copper II acetate monohydrate 0.002M to 0.01M. The sharpness and the intensity of the peaks indicate the well crystalline nature of the prepared nanocomposites.

4.3.3 SEM Analysis

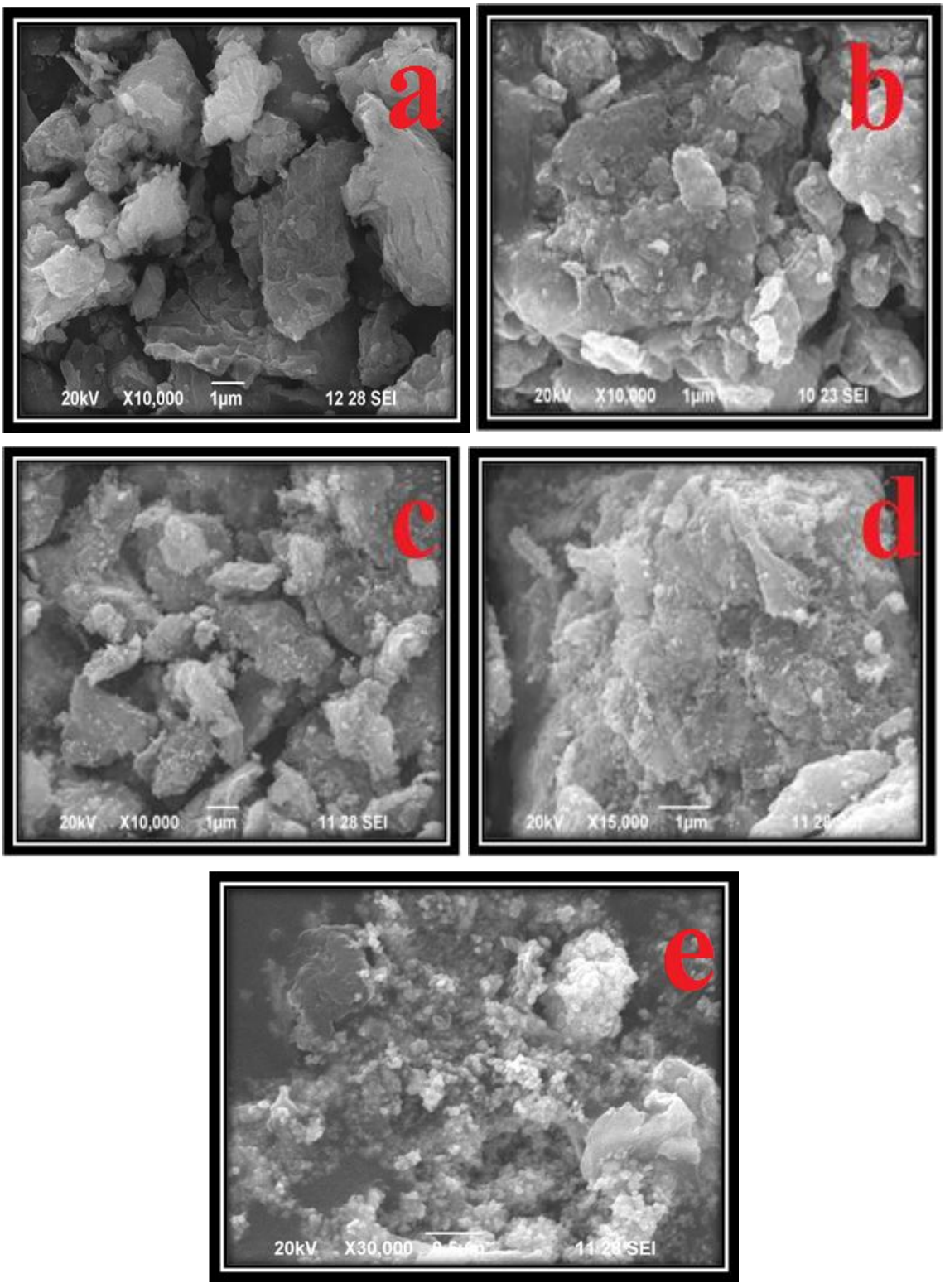

Figure 4.3 (a-e). SEM images for various concentration (a) 0.002M (b) 0.004M (c) 0.006M (d) 0.008M and (e) 0.01M of copper oxide nanoparticles incorporated on rGO/CS nanocomposites.

The morphological surface of the prepared nanocomposites is characterized using scanning electron microscope analysis. Scanning electron micrograph of various concentrations 0.002 M, 0.004 M, 0.006 M, 0.008 M and 0.01 M of copper oxide nanoparticles incorporated on rGO/CS nanocomposites are as shown in the Figure 4.3 (a-e). It is observed from the Figure 4.3 (a-e) that the spherical shaped copper oxide nanoparticles are found to be distinct, uniform and well dispersed on the surface of wrinkled rGO/CS nanosheets. The surface of the prepared nanocomposites is found to be rough, which depicts that chitosan is well functionalized and acts as a host guest material that helps in uniform dispersion of copper oxide nanoparticles on its surface [15-16].

It is further observed that on increasing the concentration of copper II acetate monohydrate from 0.002M to 0.008M, the number of nanoparticles dispersed on the surface of rGO/CS also increases. Thus on further increase in the concentration of copper II acetate monohydrate (0.01M) the nanoparticles are found to be aggregated which indicates that due to heavy loading of copper oxide nanoparticles, chitosan loses its ability to form stable nanoparticles that leads to aggregation of nanoparticles on the surface of chitosan blended wrinkled reduced graphene oxide nanosheets . Moreover due to aggregation of nanoparticles it loses its electrocatalytic property. Hence, these results clearly depict that 0.008M concentration of copper II acetate monohydrate has large surface area with uniform distribution of copper oxide nanoparticles that can be applied for the electrochemical detection of p-AP.

4.3.4 EDAX analysis

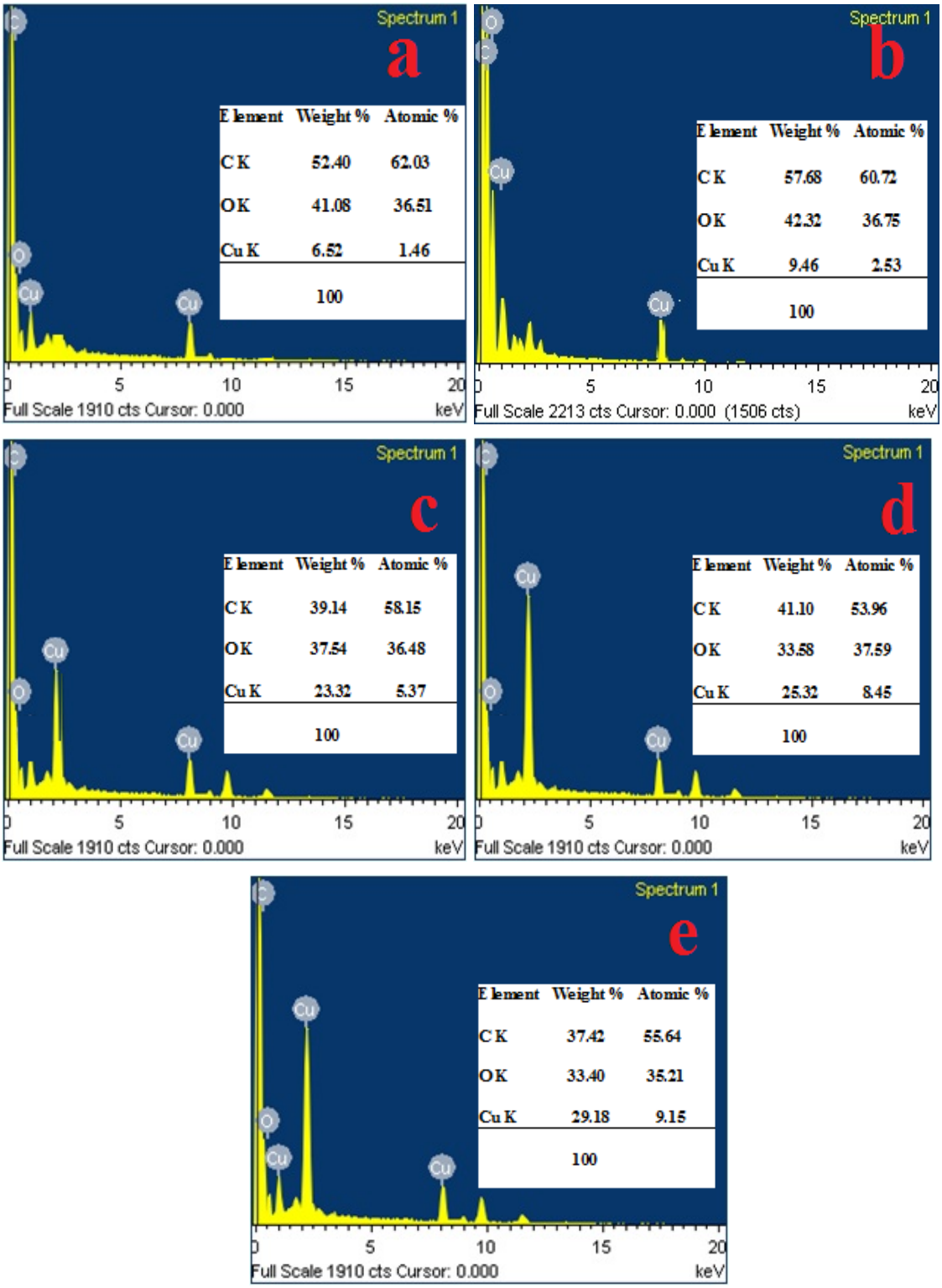

Figure 4.4.(a-e). EDAX analysis of various concentration (a) 0.002M (b) 0.004M (c) 0.006M (d) 0.008M and (e) 0.01M of copper oxide nanoparticles incorporated on rGO/CS nanocomposites.

Energy dispersive analysis of X-rays (EDAX) is carried out to determine the elemental composition and purity of the prepared nanocomposites. The spectrum is recorded in the range between 0 and 20 KeV binding energy. Figure 4.4 (a-e) depicts the EDAX analysis for various concentration 0.002M, 0.004M, 0.006M, 0.008M and 0.01M **o**f copper oxide nanoparticles embellished on rGO/CS nanocomposites. Figure 4.4 (a-e) shows the quantitative presence of carbon, oxygen and copper without any impurities that confirms the formation of rGO/CS/CuO nanocomposites [17-18]. The atomic and weight percentage of carbon, oxygen and copper for various concentration of rGO/CS/CuO nanocomposites are tabulated and shown in the inset of the Figure 4.4. It shows that the atomic and weight percentage of cu increases on increasing the concentration of copper (II) acetate which could be evidenced from SEM analysis.

4.3.5 HR-TEM Analysis

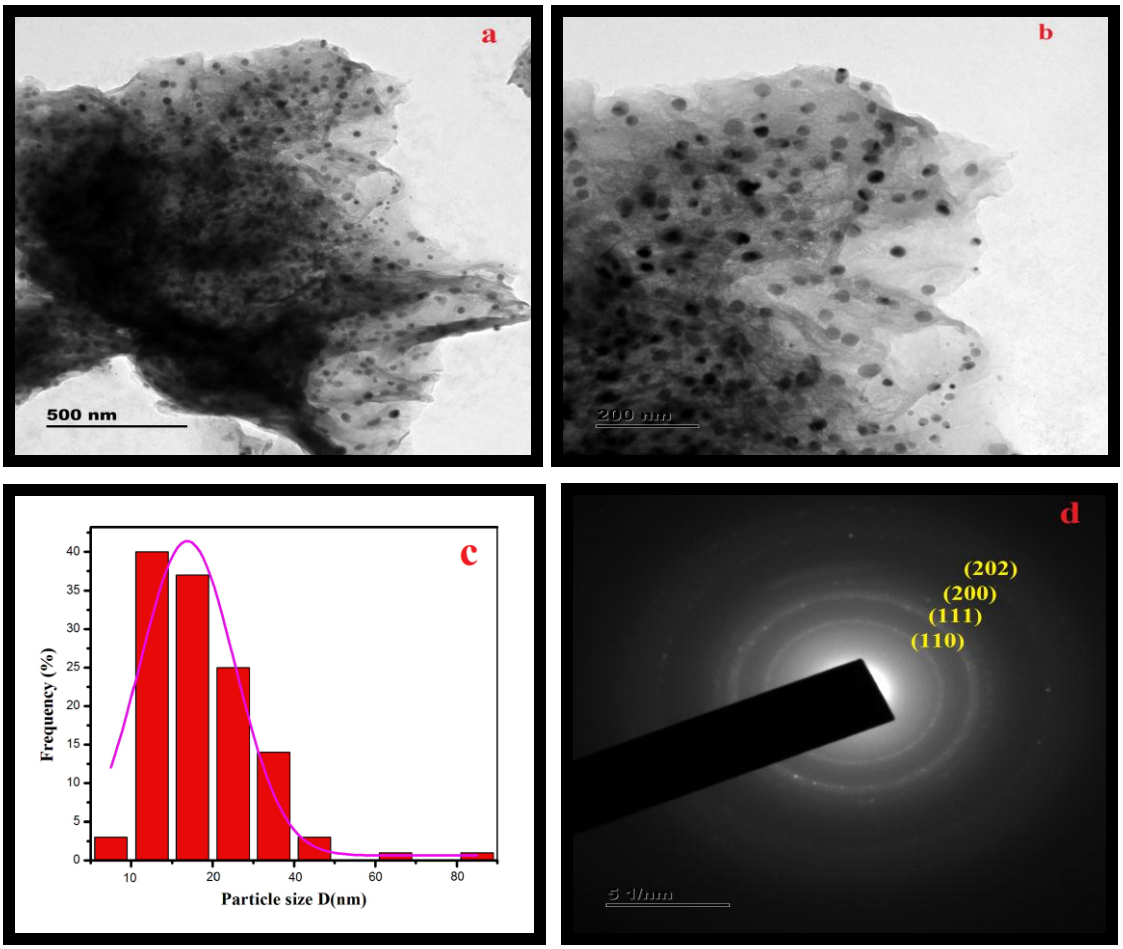

Figure 4.5(a-b) TEM images for different magnifications and (c) Particle size distribution histogram of rGO/CS/CuO nanocomposites (d) SAED pattern for 0.008M of copper oxide nanoparticles incorporated on rGO/CS nanocomposites

Figure 4.5(a-b) shows the TEM images for different magnifications of 0.008M of copper oxide nanoparticles decorated on the surface of rGO/CS nanocomposites. Figure 4.5 (a-b) depicts that the formed rGO/CS is of wrinkled, transparent and thin sheets. The spherical shaped copper oxide nanoparticles are found to be uniformly distributed and closely anchored onto the surface and edges of reduced graphene oxide/chitosan nanosheets. The copper oxide nanoparticles are homogeneously distributed without any agglomeration due to the hydrophilic and high adsorption property of chitosan. Figure 4.5 (c) shows the particle size distribution histogram of prepared nanocomposites [19]. The size distribution of the CuO nanoparticles is varied in the range of 10-50 nm with the mean diameter of 17 nm.

Figure 4.5 (d) shows the SAED pattern of 0.008M of copper oxide nanoparticles incorporated on rGO/CS nanocomposites. It is observed that four distinct diffraction rings are indexed as (110), (111), (200) and (202) that correspond to the monoclinic phase of copper oxide nanoparticles as evidenced from XRD analysis [20]. Thus the obtained distinct rings with bright spots confirm the polycrystalline nature of the prepared nanocomposites.

4.4 ELECTROCHEMICAL INVESTIGATION OF p-AMINOPHENOL

The synthesized rGO/CS/CuO nanocomposites is further investigated for the electrochemical sensing of p-AP. Based on the characterization studies, it is observed that 0.008 M of CuO nanoparticles embedded rGO/CS nanocomposites is found to be the best electrode material for the electrochemical investigation of p-AP. The electrocatalytic effect of p-AP at 0.008 M of rGO/CS/CuO nanocomposites is studied using cyclic voltammetry and various parameters such as the effect of electrolyte and the effect of scan rate are also studied.

4.4.1 Electrochemical response of p-aminophenol

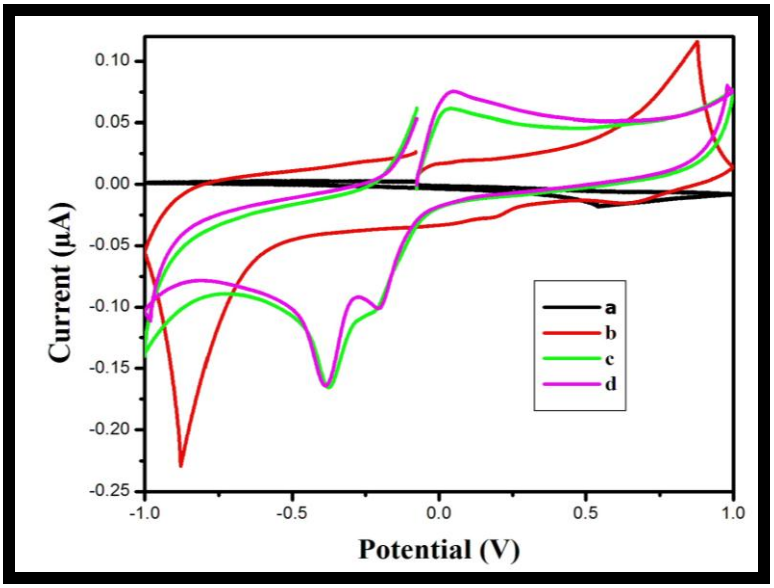

Figure 4.6 (a-d) Cyclic voltagramm curve for (a) GO/GCE (b) rGO/CS/GCE (c) rGO/CuO/GCE and (d) rGO/CS/CuO/GCE in the presence of 50µM of p-Aminophenol in 0.1 M Phosphate Buffer Solution (PBS : pH 5) at a scan rate of 20 mV s^{-1}

The electrochemical investigation of prepared rGO/CS/CuO nanocomposites towards the detection of p-AP is investigated using cyclic voltammetry Figure 4.6 (a-d) shows the cyclic voltagramm curve for GO/GCE, rGO/CS/GCE, rGO/CuO/GCE and rGO/CS/CuO/GCE in the presence of 50µM of p-Aminophenol in 0.1 M Phosphate Buffer Solution (PBS : pH 5) at a scan rate of 20 mV s^{-1}. It is observed from the Figure 4.6 (a) that in presence of 50µM of p-AP, no redox peaks is observed for GO modified GCE (GO/GCE) which depicts that GO is not active towards the detection of p-AP. But from the Figure 4.6 (b) that a pair of sluggish redox peak current of p-AP is observed at a potential of about E_{pa} = 0.02 V and E_{pc} = 0.18 V for rGO/CS modified GCE. In contrary due to excellent conductivity and the catalytic ability of rGO and copper oxide nanoparticles, a pair of redox peaks of p-AP is observed at potential of about E_{pa} = 0.036 V and E_{pc} = -0.038 V with the redox peak current of about I_{pa} = 0.05 µA and I_{pc} = -0.15 µA for rGO/CuO nanocomposites modified GCE as depicted in the Figure 4.6 (c). But rGO/CS/CuO

nanocmpositesshowed a pair of well defined redox peaks at a potential of about about E_{pa} = 0.036 V and E_{pc} = -0.038 V with the redox peak current of about I_{pa} = 0.07 µA and I_{pc} = -0.16 µA. This shows that the redox peak current of rGO/CS/CuO nanocomposites is remarkably higher than that of both rGO/CS and rGO/CuO nanocomposites [21]. Thus the enhanced redox peak current for rGO/CS/CuO nanocomposites is due to the large surface area of rGO and uniform dispersion of CuO nanoparticles in chitosan matrix that helps in accommodation of p-AP on the surface of rGO/CS/CuO modified GCE which leads to the high electron transfer rate between p-AP and the rGO/CS/CuO modified GCE. Hence, these results demonstrates that the eelctrocatalytic activity of p-AP is highly promoted on rGO/CS/CuO modified GCE and the enhanced electrocatalytic activity is due to the excellent synergetic effect between rGO, CS and CuO which provides an efficient microenvironment for the electrochemical detection of p-AP.

4.4.2 Effect of pH

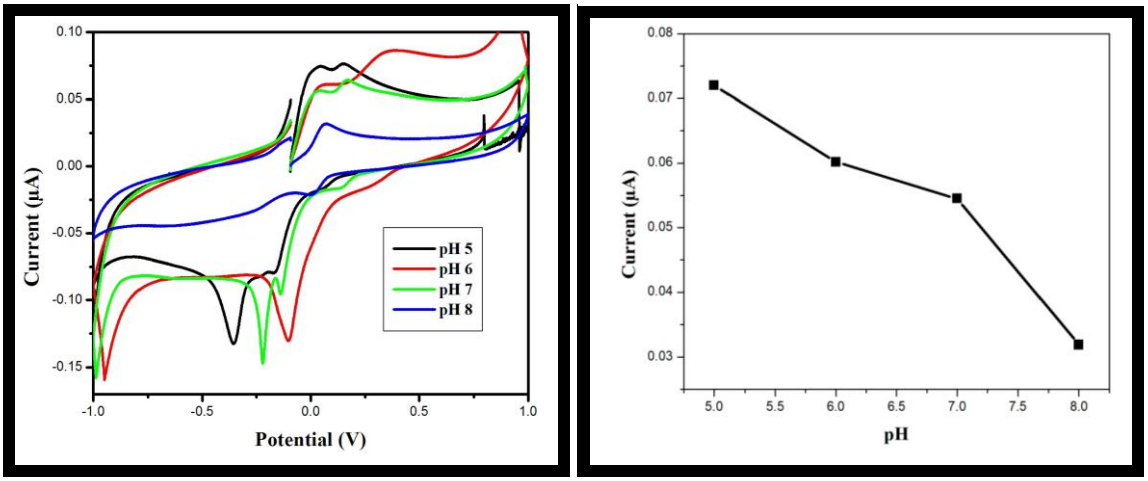

Figure 4.7 (a-b) Effect of pH on the redox peak current of 150 µM of p-AP and its linearity

The phenol compounds are greatly involved in the proton transfer of electrochemical redox process and hence the electrochemical response of phenol compounds can be affected by the pH of PBS solution. Figure 4.7 (a-b) shows the cyclic voltagramm curves for 0.008 M of rGO/CS/CuO/GCE towards the detection of 150 µM p-AP at various pH 5, 6, 7 and 8 of PBS solution in the potential range of -1 V to +1 V. It is observed from the Figure 4.7 (a) that redox peak current increases

for pH 5 of PBS solution. With further increase in pH 6 to 8 both the I_{pa} and I_{pc} gets decreases. Since the electrochemical redox process is directly involved in proton transfer, for lower pH equal number of protons and electrons are directly involved in electrochemical reaction, but for higher pH of PBS solution the number of protons involved in transfer gets decreases thus leading to decrease in redox peak current [22]. Hence, this result demonstrates that 0.1M of phosphate buffer solution (PBS) at pH 5.0 is used for electrochemical investigation of p-AP at rGO/CS/CuO/GCE due to its sensitive determination of p-AP.

4.4.3 Effect of scan rate

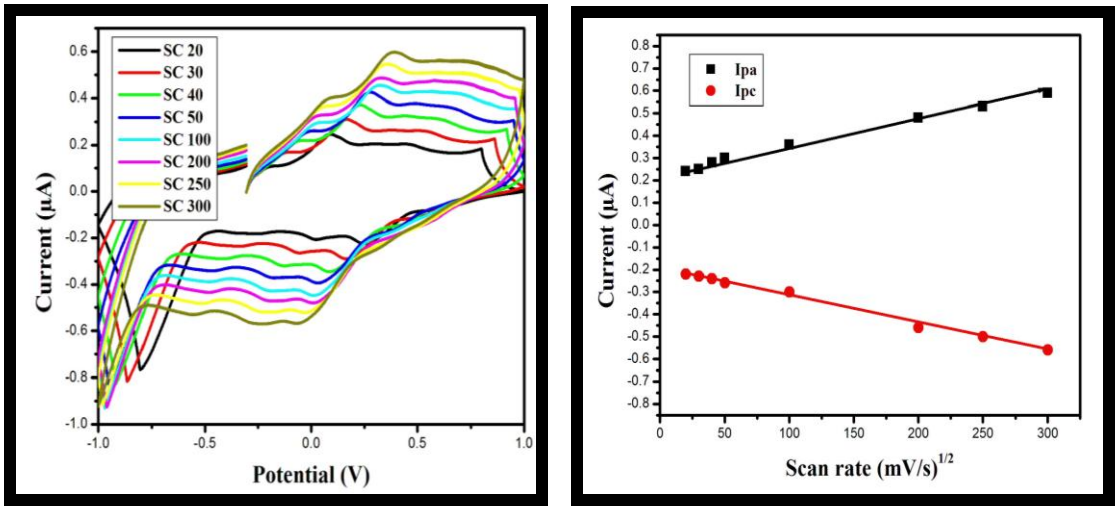

(a) **(b)**

Figure 4.8 (a-b) Cyclic voltagramm curve for effect of scanrate and its linear relationship for 150µM of p-AP in pH 5 of PBS solution

The reaction mechanism is further investigated by studying the effect of scan rate on the redox peak currents of p-AP at the rGO/CS/CuO modified GCE by cyclic voltammetry. Figure 4.8 (a-b) shows the cyclic voltagramm curves for 130µM of p-AP at pH 5 of 0.1 M of PBS solution under various scan rates for 0.008 M of rGO/CS/CuO nanocomposite modified GCE. It is observed from the Figure 4.8 (a) that the intensity of cathodic and anodic peak currents increases continuously with the increased scan rate indicating that the redox peak current of p-AP is linearly proportional to the scan rate. It is further observed that the anodic peak potential shifts positively and the cathodic peak potential shifts negatively. Figure 4.8 (b) depicts a good linear relationship between the redox peak current of p-AP and the

scan rate. It is found that for higher scan rate the electron transfer rate is also higher, resulting in the distortion of shape of redox peak currents [23]. This result demonstrates that the redox reaction of p-AP at rGO/CS/CuO nanocomposite modified GCE is diffusion controlled process.

4.4.4 Effect of analyte concentration

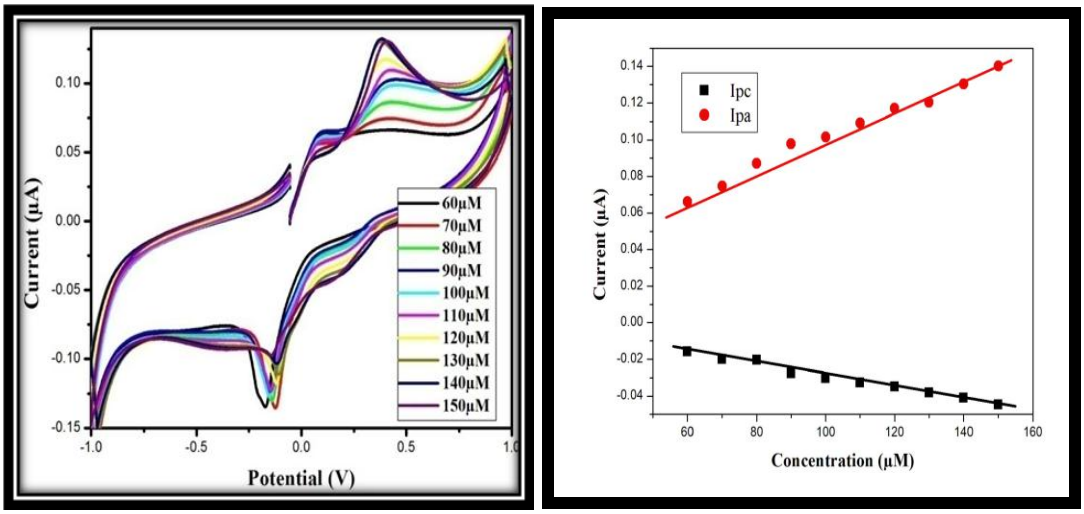

(a) **(b)**

Figure 4.9 (a-b) Cyclic voltagramm curves for 0.008M of rGO/CS/CuO/GCE towards the detection of various concentrations of p-AP in pH 5 of PBS solution at 20mV/s scan rate

Under optimized conditions the quantitative determination of p-AP is carried out in 0.1 M PBS (pH-5) at 20mV/s scan rate. Figure 4.9 (a-b) shows the cyclic voltammetric response of various concentration of p-AP at the 0.008 M of rGO/CS/CuO modified glassy carbon electrode in 0.1 M of phosphate buffer solution (PBS) at the scan rate of 20 mV/s. The electrode potential is set between -1.0 V to +1.0 V. It is observed from Figure 4.9 (a) that by increasing the concentration of p-AP, the cathodic and anodic peak current of p-AP also increases. Figure 4.9 (b) shows the relationship between the peak current response and the concentrations of p-AP. It is evident from the Figure 4.9 (a-b) that the oxidation and reduction peak current of p-AP increases linearly with the increase in concentration of p-AP. The wide linearity range is observed in the range of 60 to 150 µM [24].

4.5 CONCLUSION

This chapter deals with the facile synthesis of various concentrations (0.002 M, 0.004 M, 0.006 M, 0.008 M and 0.01 M) of copper oxide nanoparticles embedded on reduced graphene oxide/chitosan nacomposites. The rGO/CS/CuO nanocomposites are successfully synthesized by chemical reduction method. The prepared nanocomposites are characterized by XRD, FT-IR, SEM, EDAX, TEM and SAED analysis. The structural analysis revealed that the crystallite size of the copper oxide nanoparticles is in the range from 9.16 nm to 18.5 nm and increases with increase in concentration of copper (II) acetate. SEM and TEM reveals that the spherical shaped copper oxide nanoparticles are homogeneously distributed on the surface of rough, thin, wrinkled reduced graphene oxide/chitosan nanosheets. Elemental analysis reveals the quantitative presence of carbon, oxygen and copper without any impurities. The electrochemical performance of the prepared nanocomposites towards the detection of p-AP is studied using cyclic voltammetry. Hence, 0.008 M molarity of rGO/CS/CuO nanocomposite modified GCE shows excellent electrocatalytic activity towards the detection of p-AP due to its uniform dispersion of CuO nanoparticles on the large surface area of rGO/CS that leads to good electron transfer rate between p-AP and rGO/CS/CuO nanocomposite modified GCE. The maximum redox peak current of 0.008M of rGO/CS/CuO nanocomposite is 0.18µA is observed for pH 5 and the linear range of detection around 60µM to 150µM.

REFERENCES

1. PolymerYong Liu, Kai Yan, BinWang, Changzhu Yang and Jingdong Zhang, An Electrochemical Sensor for Selective Detection of *p*-Aminophenol Using Hemin-Graphene Composites and Molecularly Imprinted, Journal of The Electrochemical Society, 164 (14) B776-B780, (2017).

2. Junjuan Qian, Depeng Zhang, Lirong Liu, Yinhui Yi, Mwenze Nkulu Fiston,Odoom Jibrael Kingsford and Gangbing Zhu, Carbon Spheres Wrapped with Molybdenum DisulfideNanostructure for Sensitive Electrochemical Sensing of 4-aminophenol, Journal of The Electrochemical Society, 165 (11) B491-B497 (2018)

3. S. Praveen Kumar, K. Giribabu, R. Manigandan, S. Munusamy, S. Muthamizh , A. Padmanaban, T. Dhanasekaran, R. Suresh, V. Narayanan, Simultaneous determination of paracetamol and 4-aminophenol based on poly(chromium Schiff base complex) modified electrode at nanomolar levels, Electrochimica Acta, vol.no.194 pg.no.116–126, (2016)

4. O. Akgul , U. Alver and A. Tanrıverdi, Characterization of graphene oxide produced by Hummers method and its supercapacitor applications, AIP Conference Proceedings 1722, 280001, doi: 10.1063/1.4944280, (2016)

5. Abdullahi Mohamed Farah, Force Tefo Thema and Ezekiel Dixon Dikio, Electrochemical Detection of Hydrogen Peroxide Based on Graphene Oxide/Prussian Blue Modified Glassy Carbon Electrode, Int. J. Electrochem. Sci., 7 5069 – 5083, (2012).

6. Mona Mohseni and Hasan Tahermansouri, Development of a graphene oxide/chitosan nanocomposite for the removal of picric acid from aqueous solutions: study of sorption parameters, https://doi.org/10.1016/j.colsurfb. 2017.10.019, (2017).

7. Chandrama Sarkar and Swapan K. Dolui, Synthesis of copper oxide/reduced graphene oxide nanocomposite and its enhanced catalytic activity towards reduction of 4-nitrophenol, RSC Adv, 5, 60763, (2015)

8. Antonella Arena, Graziella Scandurra and Carmine Ciofi, Copper Oxide Chitosan Nanocomposite:Characterization and Application in Non-Enzymatic Hydrogen Peroxide Sensing, Sensors, 17, 2198, (2017)

9. Jonghoon Choi, Hana Oh, Sang-Wook Han, Seokhoon Ahn, Jaegeun Noh, Joon B.Park, Preparation and characterization of graphene oxide supported Cu, Cu2O and CuO nanocomposites and their high photocatalytic activity for organic dye molecule, S1567-1739(16)30335-2, (2016)

10. S.Selvam, B.Balamuralitharan, S.Jegatheeswaran, Mi-Young Kim, S.N.Karthick J.Anandha Raj, P.Boomi, M.Sundrarajan, K.Prabakar, Hee-Je Kim, Electrolyte imprinted graphene oxide-Chitosan chelate with copper crosslinked composite electrodes for intense cyclic stable flexible supercapacitors

11. Ajay Gupta, Ramen Jamatia, Ranjit A. Patil, Yuan-Ron Ma and Amarta Kumar Pal, Copper Oxide/Reduced Graphene Oxide Nanocomposite-Catalyzed Synthesis of Flavanones and Flavanones with Triazole Hybrid Molecules in One Pot: A Green and Sustainable Approach, ACS Omega, 3, 7288−7299, (2018)

12. Anshu Dandia, Sarika Bansal, Ruchi Sharma, Kuldeep S. Rathore and Vijay Parewa, Microwave-assisted nanocatalysis: A CuO NPs/rGO composite as an efficient and recyclable catalyst for the Petasis-borono–Mannich reaction, RSC Adv, 8, 30280, (2018)

13. Sudhakar Y. N, Hemant H, Nitinkumar S. S, Poornesh, P and Selvakumar M, Green synthesis and electrochemical characterization of rGO–CuO nanocomposites for supercapacitor applications, Ionics, 23(5), 1267–1276, doi:10.1007/s11581-016-1923-7 (2016).

14. Jian Song, Lin Xu, Chunyang Zhou, Ruiqing Xing, Qilin Dai, Dali Liu and Hongwei Song, Synthesis of Graphene Oxide Based CuO Nanoparticles Composite Electrode for Highly Enhanced Nonenzymatic Glucose Detection, ACS Appl. Mater. Interfaces, 5, 12928−12934, (2013)

15. Zhao Y, Song X, Song Q and Yin Z, A facile route to the synthesis copper oxide/reduced graphene oxide nanocomposites and electrochemical detection of catechol organic pollutant. CrystEngComm, 14(20), 6710.doi:10.1039/c2ce25509j, (2012).

16. S. Logpriya, V. Bhuvaneshwari, D. Vaidehi, R. P. SenthilKumar, R. S. Nithya Malar, B. Pavithra Sheetal, R. Amsaveni, M. Kalaiselvi, (2018) Preparation and characterization of ascorbic acid‐mediated chitosan–copper oxide nanocomposite for anti‐microbial, sporicidal and biofilm‐inhibitory activity, Journal of Nanostructure in Chemistry, vol. 8, pg.no:301–309 (SEM)

17. Upasana Gulati, U. Chinna Rajesh, and Diwan S. Rawat, RGO@CuO Nanocomposites From A Renewable Copper Mineral Precursor: A Green Approach For Decarboxylative C(sp3)-H Activation Of Proline Amino Acid To Afford Value-Added Synthons ACS Sustainable Chemistry & Engineering, DOI: 10.1021/ acssuschemeng.8b01376, (2018)

18. Gangyong Li, Mingjun Jing, Zhengu Chen, Binhong He, Minjie Zhou and Zhaohui Hou, Self-assembly of porous CuO nanospheres decorated on reduced graphene oxide with enhanced lithium storage performance, RSC Adv, 7, 10376–10384, (2017)

19. Suresh Sagadevan, Zaira Zaman Chowdhury, Mohd. Rafie Bin Johan, Fauziah Abdul Aziz, Emee Marina Salleh, Anil Hawa & Rahman F. Rafique A one-step facile route synthesis of copper oxide/ reduced graphene oxide nanocomposite for supercapacitor applications, Journal of Experimental Nanoscience, Vol. 13, no. 1, 284–295, (2018).

20. Afshin Pendashteha, Mir Fazlollah Mousavia and Mohammad Safi Rahmanifar, Fabrication of anchored copper oxide nanoparticles on graphene oxide nanosheets via an electrostatic coprecipitation and its application as supercapacitor, Electrochimica Acta, 88 347– 357, (2013) tem

21. Youcheng Zhao, Xinyu Song, Qisheng Song and Zhilei Yin, A facile route to the synthesis copper oxide/reduced graphene oxide nanocomposites and electrochemical detection of catechol organic pollutant, CrystEngComm, 14, 6710–6719, (2012)

22. Dong Sun, Xiaokun Li, Huajie Zhang and Xiafeng Xie, An electrochemical sensor for p-aminophenol based on the mesoporous silica modified carbon paste electrode, Intern. J. Environ. Anal. Chem. Vol. 92, issue.3, pg.no.324–333, (2012)

23. Yang Fan, Jin-Hang Liu, Chun-Peng Yang, Meng Yu, Peng Liu, Graphene–polyaniline composite film modified electrode for voltammetric determination of 4-aminophenol, Sensors and Actuators B, vol.no.157, pg.no: 669– 674, (2011).

24. Huijuan Wang, Siyu Zhang, Shufang Li, and Jianying Qu, Electrochemical sensor based on palladium-reduced graphene oxide modified with gold nanoparticles for simultaneous determination of acetaminophen and 4-aminophenol, (2017)